Letter

Observation of the electromagnetic Dalitz transition $h_c \to e^+e^-\eta_c$

M. Ablikim *et al.*[*]
(BESIII Collaboration)

(Received 5 July 2024; revised 12 October 2024; accepted 18 November 2024; published 12 December 2024)

Using $(27.12 \pm 0.14) \times 10^8$ $\psi(3686)$ decays and data samples of e^+e^- collisions with $\sqrt{s}$ from 4.130 to 4.780 GeV collected with the BESIII detector, we report the first observation of the electromagnetic Dalitz transition $h_c \to e^+e^-\eta_c$ with a statistical significance of 5.4σ. We measure the ratio of the branching fractions $\frac{\mathcal{B}(h_c\to e^+e^-\eta_c)}{\mathcal{B}(h_c\to\gamma\eta_c)}$ separately for the h_c samples produced via $\psi(3686) \to \pi^0 h_c$ and $e^+e^- \to \pi^+\pi^- h_c$. The average ratio is determined to be $(0.59 \pm 0.10(\text{stat}) \pm 0.04(\text{syst}))\%$, where the uncertainty includes both statistical and systematic components.

DOI: 10.1103/PhysRevD.110.L111101

The charmonium system, composed of a charm quark bound to an anticharm quark ($c\bar{c}$), has played an important role in our understanding of the fundamental theory of the strong interactions between quarks and gluons, quantum chromodynamics (QCD). In the last decade, the electromagnetic (EM) Dalitz decays of charmonia, due to their crucial role as a ideal avenue for probing the intrinsic structure of charmonia and unraveling the fundamental mechanisms underlying the interactions between photons and hadrons [1,2], have captured significant interest both experimentally and theoretically [3]. All charmonium states below the open-charm $D\bar{D}$ threshold have been observed experimentally and are well described by potential models [4]. However, our knowledge of the P-wave singlet charmonium state, the $h_c(^1P_1)$, is sparse compared to other charmonium resonances. Its best-measured decay mode is the radiative transition $h_c \to \gamma\eta_c$, whose branching fraction is about 60%, while the sum of all other known h_c decay branching fractions is less than 3% [5]. Therefore, there is still much to be learned about the decays of this state.

Searching for new h_c decay modes is important to constrain theoretical models in the charmonium region [4]. In particular, electromagnetic (EM) Dalitz decays, such as $h_c \to e^+e^-\eta_c$ in which a virtual photon internally converts into an e^+e^- pair, play an important role in revealing the structure of hadrons and their interactions with photons [2]. The first observation of the Dalitz decay of h_c, attributed to the emergence of electromagnetic structure at the $h_c - \eta_c$ transition vertex, offers a favorable opportunity for exploring its transition form factors in the next-generation experiment.

Due to the absence of allowed $E1$ (electric dipole) or $M1$ (magnetic dipole) radiative transitions from the $\psi(3686)$, the production of the h_c proceeds through the isospin-violating decay $\psi(3686) \to \pi^0 h_c$ and is therefore highly suppressed. However, in e^+e^- machines, the h_c can also be produced in the process $e^+e^- \to \pi^+\pi^- h_c$, which is found to have a comparable production rate with that of $\psi(3686) \to \pi^0 h_c$ [6]. In this case, the large data samples of e^+e^- annihilations collected with the BESIII detector offer an excellent opportunity to explore the EM Dalitz decays of the h_c using a combination of h_c samples produced in both the processes $\psi(3686) \to \pi^0 h_c$ and $e^+e^- \to \pi^+\pi^- h_c$.

In this paper, we report the first observation of the charmonium EM Dalitz decay $h_c \to e^+e^-\eta_c$ via the processes $\psi(3686) \to \pi^0 h_c$ (Mode I) and $e^+e^- \to \pi^+\pi^- h_c$ (Mode II). For Mode I, we use a sample of $(27.12 \pm 0.14) \times 10^8$ $\psi(3686)$ events [7]. For Mode II, we use e^+e^- collision data samples taken at center-of-mass energies 4.130, 4.160, 4.210, 4.230, 4.237, 4.246, 4.260, 4.270, 4.280, 4.290, 4.315, 4.340, 4.360, 4.380, 4.400, 4.420, 4.440, 4.740 and 4.780 GeV (called "XYZ data" hereafter), corresponding to a total integrated luminosity of 10507.44 pb^{-1} [8–11]. The measurement of the ratio $\frac{\mathcal{B}(h_c\to e^+e^-\eta_c)}{\mathcal{B}(h_c\to\gamma\eta_c)}$ is also presented for the first time, where η_c is not reconstructed to improve efficiency, and the recoil system is employed for the investigation of both the η_c and h_c, following the same approach as the previous BESIII and CLEO experiments [12–15]. The advantage of comparing these two h_c decay channels is that parts of the systematic uncertainties due to tracking, particle identification (PID), the branching fraction of $\psi(3686) \to \pi^0 h_c$, the cross section of $e^+e^- \to \pi^+\pi^- h_c$, and the number of $\psi(3686)$ events cancel in the ratio.

[*]Full author list given at the end of the Letter.

The design and performance of the BESIII detector is described in detail in Refs. [16,17]. Simulated samples including the inclusive and exclusive ones produced with the GEANT4-based [18] Monte Carlo (MC) package, which includes the geometric description of the BESIII detector and the detector response, are used to determine the detection efficiency and to estimate the backgrounds. The productions of the h_c resonance from $\psi(3686) \to \pi^0 h_c$ and $e^+e^- \to \pi^+\pi^-$ are simulated by HELAMP and PHSP model, respectively, both of them from the MC event generator EVTGEN [19,20]. The $E1$ transition $h_c \to \gamma\eta_c$ is modeled with EVTGEN [19,20], with an angular distribution of $1+\cos^2\theta$ in the h_c rest frame, while the EM Dalitz decay $h_c \to e^+e^-\eta_c$ is simulated by a new generator as described in the Supplemental Material [20]. The known decay modes of the η_c resonance are generated by EVTGEN [19,20] with branching fractions set to the world average values [5], and by LUNDCHARM [21] for the remaining unknown decays.

For both Mode I and Mode II, candidate charged tracks and EM showers are required to satisfy the following common selection criteria. (i) Charged tracks are reconstructed using the tracking information from the main drift chamber (MDC). The distance of the closest approach of every charged track to the e^+e^- interaction point is required to be within ± 10 cm along the beam direction and within 1 cm in the plane perpendicular to the beam direction. The polar angle θ between the direction of a charged track and that of the beam must satisfy $|\cos\theta| < 0.93$ for an effective measurement in the active volume of the MDC. The combined information of the specific ionization energy loss ($\mathrm{d}E/\mathrm{d}x$) in the MDC and the time of flight (TOF) in the TOF system is used to calculate PID confidence levels (CLs) for the electron, pion and kaon hypotheses. The particle type with the highest PID CL is assigned to each track. (ii) EM showers are reconstructed from clusters of deposited energy in the electromagnetic calorimeter (EMC). The shower energies of photon candidates in the EMC must be greater than 25 MeV in the barrel region ($|\cos\theta| < 0.80$) or greater than 50 MeV in the end cap regions ($0.86 < |\cos\theta| < 0.92$). Showers located in the transition regions between the barrel and the end cap regions are excluded. To avoid showers caused by charged particles, a photon candidate has to be separated by at least 10° from any charged track, as specified by the BESIII detector optimization for photon initial selection [22–27]. In order to suppress electronic noise and energy depositions that are unrelated to the event, the EMC time t of the photon candidates must be in coincidence with collision events within the range $0 \le t \le 700$ ns.

For Mode I, pairs of photons are accepted as π^0 candidates in $\psi(3686) \to \pi^0 h_c$ if their reconstructed invariant mass satisfies $M_{\gamma\gamma} \in [120, 145]$ MeV$/c^2$. To improve the signal-to-noise ratio, photons related to π^0 candidates have to be detected in the barrel EMC region with an energy greater than 40 MeV. To reject background, a one-constraint (1C) kinematic fit is performed to the photon pairs, constraining their invariant mass to the nominal π^0 mass M_{π^0} [5], and the best π^0 candidate is chosen based on the smallest χ^2_{1C} value. Background events from $\psi(3686) \to \pi^+\pi^- J/\psi$ and $\psi(3686) \to \gamma\gamma J/\psi$ are suppressed by requiring the recoil mass of each $\pi^+\pi^-$ ($\gamma\gamma$) pair in an event to be outside the range of $M_{J/\psi} \pm 7$ MeV$/c^2$ ($M_{J/\psi} \pm 30$ MeV$/c^2$), where $M_{J/\psi}$ is the nominal J/ψ mass [5].

For the decay $h_c \to \gamma\eta_c$, the dominant background for the $E1$ photon is from π^0 decay. To suppress this background, we combine the $E1$ photon candidate with all other photons in the event and reject the event if any combination has an invariant mass within 15 MeV$/c^2$ of the nominal π^0 mass.

For the decay $h_c \to e^+e^-\eta_c$, candidates are required to have at least two charged tracks identified as an electron and a positron. An additional criterion $0.5 < E/p < 1.2$ is applied to the track with higher momentum in the e^+e^- pair to further improve the electron identification, where E and p refer to the energy deposition in the EMC and the momentum measured with the MDC, respectively.

In order to suppress background from $\pi^0 \to \gamma e^+e^-$ in the $\psi(3686) \to \pi^0 h_c, h_c \to e^+e^-\eta_c$ decay, the invariant mass of $e^+e^-\gamma'$ is required to be outside the range of $M_{\pi^0} \pm 15$ MeV$/c^2$, where γ' is either photon from the π^0 candidate. To remove the background from $h_c \to \gamma\eta_c$, where the photon subsequently converts into an e^+e^- pair in the beam pipe or in the inner wall of the MDC, a photon conversion (PC) finder [28] is applied to all e^+e^- pairs. The PC point is reconstructed using the two charged trajectories in the x–y plane, which is perpendicular to the beam line. The PC length δ_{xy} is defined as the distance between the PC point and (0, 0, 0) point in the x–y plane. Photon conversion events accumulate at $\delta_{xy} = 3$ cm and $\delta_{xy} = 6.5$ cm corresponding to the positions of the beam pipe and the inner wall of the MDC. A detailed study [28] illustrates that the distributions of δ_{xy} for data and MC simulations are consistent with each other. By requiring $\delta_{xy} < 2$ cm, background from photon conversion is removed.

For Mode II, candidate events are required to have at least two tracks with opposite charge identified as two pions, while the requirements for the e^+e^- pair from the decay $h_c \to e^+e^-\eta_c$ and the requirements for the $E1$ photon from the decay $h_c \to \gamma\eta_c$ are the same as those described above for Mode I.

To select the η_c in Mode I, we require that the energy of the e^+e^- pair from $h_c \to e^+e^-\eta_c$ and the energy of the γ from $h_c \to \gamma\eta_c$ to be in the range [470, 540] MeV. To select the η_c in Mode II, we require the masses recoiling against the $\pi^+\pi^-e^+e^-$ and $\pi^+\pi^-\gamma$ systems to be within the η_c mass window $[2.92, 3.08]$ GeV$/c^2$. After the above requirements, extensive examination of the $E_{e^+e^-}$ sideband reveals

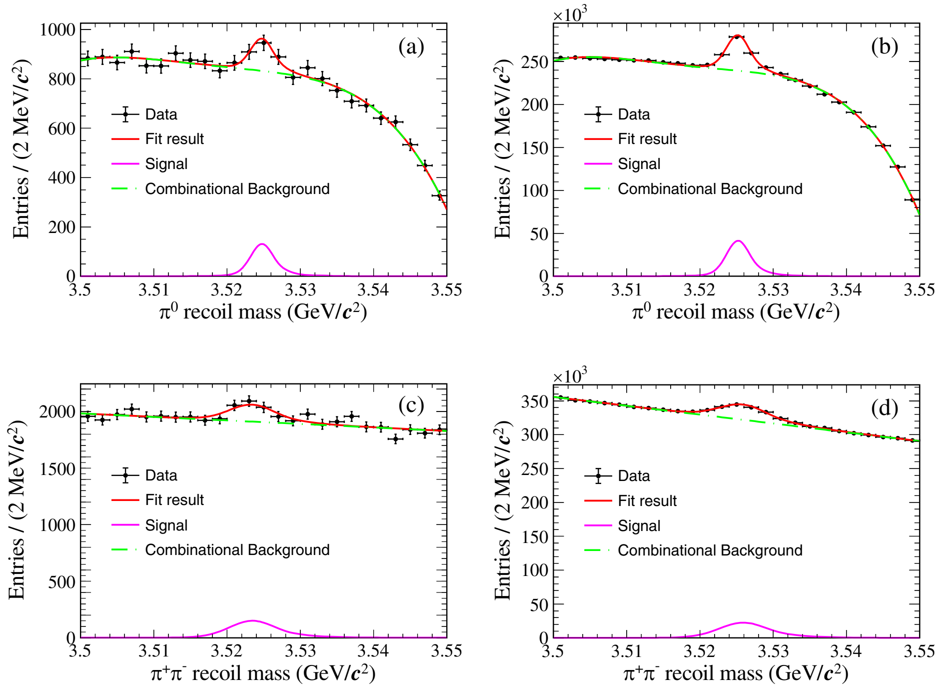

FIG. 1. (a,b) The π^0 recoil mass spectra for $\psi(3686) \to \pi^0 h_c$ with (a) $h_c \to e^+e^-\eta_c$ and (b) $h_c \to \gamma\eta_c$. (c,d) The $\pi^+\pi^-$ recoil mass spectra for $e^+e^- \to \pi^+\pi^- h_c$ with (c) $h_c \to e^+e^-\eta_c$ and (d) $h_c \to \gamma\eta_c$ selected from XYZ data. The total fit results are shown as solid red lines, the signals as solid pink lines and the backgrounds as dashed green lines.

the absence of any peaking background beneath the h_c signal. The masses recoiling against the π^0 (Mode I) and $\pi^+\pi^-$ (Mode II) systems are shown in Fig. 1. There is a prominent peak for the decays $h_c \to \gamma\eta_c$ and $h_c \to e^+e^-\eta_c$.

To evaluate the statistical significance and the signal yields of the $h_c \to e^+e^-\eta_c$ decay, we perform a simultaneous unbinned maximum likelihood fit to the π^0 and $\pi^+\pi^-$ recoil mass spectra, which are displayed in Figs. 1(a) and 1(c). The signal shapes for Mode I and Mode II are parmetrized as a common Breit-Wigner function with a fixed width of 0.78 MeV [29] and a floating resonance mass, convolved with a Crystal Ball function to account for the mass resolution effect. The parameters for the Crystal Ball function are fixed to be those obtained from the MC simulations, respectively, for the above two modes. The background shapes for Mode I and Mode II are described by a fourth-order and a first-order Chebyshev function, respectively. The fit gives a peak at (3524.72 ± 0.47) MeV/c^2, which is in good agreement with the world average value of the h_c mass [5], with a statistical significance of 5.4σ. The statistical significance is determined by the change of the log-likelihood value and the number of degrees of freedom in the fit with and without the h_c signal. To conservatively estimate the significance, the minimum one is ultimately chosen with the effects of both signal and background shapes taken into account. For the reference channel of $h_c \to \gamma\eta_c$, a simultaneous fit to the π^0 [Fig. 1(b)] and $\pi^+\pi^-$ [Fig. 1(d)] recoil mass spectra is also performed with the same signal model and the background shapes as those for the $h_c \to e^+e^-\eta_c$ decay. For the above two cases, the fit results are summarized in Table I.

Using the MC-determined efficiencies and the fitted signal yields, the ratios of the branching fractions, given in Table I, are calculated with

$$\mathcal{R} \equiv \frac{\mathcal{B}(h_c \to e^+e^-\eta_c)}{\mathcal{B}(h_c \to \gamma\eta_c)} = \frac{N^{\rm obs}_{e^+e^-\eta_c}}{N^{\rm obs}_{\gamma\eta_c}} \cdot \frac{\epsilon_{\gamma\eta_c}}{\epsilon_{e^+e^-\eta_c}}, \qquad (1)$$

where $N^{\rm obs}_{e^+e^-\eta_c}$ and $N^{\rm obs}_{\gamma\eta_c}$ represent the numbers of the $h_c \to e^+e^-\eta_c$ and $h_c \to \gamma\eta_c$ signal events from the fits, and $\epsilon_{e^+e^-\eta_c}$ and $\epsilon_{\gamma\eta_c}$ are the corresponding detection efficiencies. The measured ratios from two Modes are in reasonable agreement within two standard deviations due to the large statistical uncertainties.

All the systematic uncertainties taken into account are summarized in Table II. The tracking efficiency has been studied using the control samples of $J/\psi \to e^+e^-(\gamma_{\rm FSR})$ [30] and $J/\psi \to \rho\pi$ [31], where FSR means final-state radiation. The difference in efficiencies between data and MC simulation for electrons, positrons, and charged pions is estimated to be 1.0% for each charged track. The total

TABLE I. The fit results and the measured $\mathcal{R}$ for Mode I and Mode II.

Mode	$N^{\rm obs}_{e^+e^-\eta_c}$	$N^{\rm obs}_{\gamma\eta_c}$	$\epsilon_{e^+e^-\eta_c}$	$\epsilon_{\gamma\eta_c}$	$\mathcal{R}(\%)$
I	298 ± 76	95564 ± 1340	5.38%	7.99%	$0.46 \pm 0.12 \pm 0.05$
II	663 ± 136	99260 ± 1792	24.73%	33.12%	$0.89 \pm 0.18 \pm 0.09$

TABLE II. The systematic uncertainties (in %) in the calculation of $\mathcal{R}$. The items with and without $*$ are common and independent uncertainties, respectively. The total systematic uncertainty is obtained by adding individual contributions in quadrature for independent items and the remaining contributions after partial cancellation for common items.

	Mode I		Mode II	
Source	$e^+e^-\eta_c$	$\gamma\eta_c$	$e^+e^-\eta_c$	$\gamma\eta_c$
Charged tracks*	2.0	⋯	4.0	2.0
Photon detection*	2.0	3.0	⋯	1.0
$e^\pm$ PID*	3.2	⋯	3.2	⋯
γ conversion	1.0	⋯	1.0	⋯
π^0 reconstruction*	0.7	0.7	⋯	⋯
Form factor	1.4	⋯	1.4	⋯
Fitting range	3.7	4.7	1.8	0.1
Background shape	2.4	2.8	0.9	6.0
Background contamination	⋯	0.9	⋯	1.3
Signal shape	5.0	4.9	1.8	5.5
Energy cut	0.3	3.9	⋯	⋯
Total	11.5		9.7	

systematic uncertainty is then taken to be 1.0% times the number of selected charged tracks in each process.

The photon detection efficiency has been studied using a control sample of $J/\psi \to \rho\pi$ [31]. It is found that the detection efficiency of MC simulation is in agreement with that of data within 1.0%, which is taken as the systematic uncertainty for each photon. The total systematic uncertainty from this source is determined by the number of selected good photons in each process.

The uncertainty on electron and positron identification is studied with a control sample of radiative Bhabha scattering events $e^+e^- \to \gamma e^+e^-$. The average efficiency difference for electron and positron identification between data and MC simulation, weighted according to the polar angle and momentum distributions of the signal MC samples, is determined to be 1.6% for each of them. Thus, a systematic uncertainty of 3.2% is assigned.

We perform a study of γ conversion events with a clean control sample of $J/\psi \to \pi^+\pi^-\pi^0, \pi^0 \to \gamma e^+e^-$. The systematic uncertainty due to the γ conversion veto is estimated to be 1.0% [32], which is the relative difference of efficiencies between data and MC simulation.

The systematic uncertainty due to the $E_{e^+e^-}$ or E_γ requirements is estimated by varying the range of $E_{e^+e^-}$ and E_γ from [470, 540] MeV to [480, 540] MeV. The differences of branching fractions between different energy ranges, 0.3% and 3.9%, are taken as the systematic uncertainties from the energy cut of $h_c \to e^+e^-\eta_c$ and $h_c \to \gamma\eta_c$ in $\psi(3686)$ decays, respectively.

The uncertainty due to π^0 reconstruction is investigated using double-tag $D\bar{D}$ hadronic decay samples of $D^0 \to K^-\pi^+, K^-\pi^+\pi^+\pi^-$ versus $\bar{D}^0 \to K^+\pi^-\pi^0, K_S^0\pi^0$ [33,34]. The average data-MC difference of the π^0 reconstruction efficiencies, weighted by the momentum spectra of signal MC events, is 0.7% per π^0.

In the generator for the decay $h_c \to e^+e^-\eta_c$, the form factor $V(q^2) = \frac{1}{1-q^2/\Lambda^2}$ is used, where q^2 is the square of the invariant mass of the e^+e^- pair, and the pole mass Λ is the mass of the vector resonance near the energy scale of the decaying particle according to the vector meson dominance model [35,36]. To generate the signal MC sample, we assume that the value of Λ is $M_{J/\psi}$. In order to obtain the systematic uncertainty from the generator, we generate a new signal MC sample by changing the value of Λ to M_{h_c}. The difference of detection efficiency between these two samples gives an uncertainty of 1.4%.

The fitting range, signal and background descriptions are considered as sources of systematic uncertainty related to the fitting procedure. These uncertainties are determined by varying the fitting ranges, changing the width parameter in h_c signal shape, and varying the orders of the Chebychev functions in the fit. The maximum differences of the fit results are assigned as the systematic uncertainties from each item of the fitting procedure as shown in Table II.

To assess the contamination from the h_c decays in the absence of an intermediate η_c, the dedicated MC simulations were performed for h_c directly decaying into hadrons without η_c. It is found that the background contributions to $h_c \to e^+e^-\eta_c$ could be ignored, while the contamination to $h_c \to \gamma\eta_c$ are 0.9% and 1.3%, respectively, for Mode I and Mode II.

The systematic uncertainties from different sources and their corresponding contributions are summarized in Table II, where the total systematic uncertainties of $\mathcal{R}$ for Mode I and Mode II are calculated by assuming that the common systematic uncertainties between the two h_c decays cancel in the measurement of $\mathcal{R}$.

In summary, based on $(27.12 \pm 0.14) \times 10^8$ $\psi(3686)$ events and XYZ data, corresponding to a total integrated luminosity of 10507.44 pb^{-1} taken at center-of-mass energies between 4.130 and 4.780 GeV collected with the BESIII detector, we observe the EM Dalitz decay $h_c \to e^+e^-\eta_c$ with a statistical significance of 5.4σ. We measure the ratio $\mathcal{R} = \frac{\mathcal{B}(h_c \to e^+e^-\eta_c)}{\mathcal{B}(h_c \to \gamma\eta_c)}$ separately for samples of h_c produced in the two processes $\psi(3686) \to \pi^0 h_c$ and $e^+e^- \to \pi^+\pi^- h_c$, and the results are shown in Table I. Combining the results with the weighted least squares method from $\psi(3686)$ and XYZ data gives $\mathcal{R} = (0.59 \pm 0.10(\mathrm{stat}) \pm 0.04(\mathrm{syst}))\%$, where correlations of different sources of systematic uncertainties between the two modes are taken into account. This result provides new experimental inputs and vertex information on the interaction of charmonium states with the EM field. This is the first measurement of this branching ratio and is important to guide models in the description of charmonium decays.

The BESIII Collaboration thanks the staff of BEPCII and the IHEP computing center for their strong support. This work is supported in part by National Key R&D Program of China under Contracts No. 2020YFA0406300, No. 2020YFA0406400, No. 2023YFA1606000; National Natural Science Foundation of China (NSFC) under Contracts Nos. 11635010, 11735014, 11935015, 11935016, 11935018, 12025502, 12035009, 12035013, 12061131003, 12075250, 12075252, 12192260, 12192261, 12192262, 12192263, 12192264, 12192265, 12221005, 12225509, 12235017, 12361141819; the Chinese Academy of Sciences (CAS) Large-Scale Scientific Facility Program; the CAS Center for Excellence in Particle Physics (CCEPP); Joint Large-Scale Scientific Facility Funds of the NSFC and CAS under Contract No. U1832207; 100 Talents Program of CAS; The Institute of Nuclear and Particle Physics (INPAC) and Shanghai Key Laboratory for Particle Physics and Cosmology; German Research Foundation DFG under Contract Nos. FOR5327, GRK 2149; Istituto Nazionale di Fisica Nucleare, Italy; Knut and Alice Wallenberg Foundation under Contract Nos. 2021.0174, 2021.0299; Ministry of Development of Turkey under Contract No. DPT2006K-120470; National Research Foundation of Korea under Contract No. NRF-2022R1A2C1092335; National Science and Technology fund of Mongolia; National Science Research and Innovation Fund (NSRF) via the Program Management Unit for Human Resources & Institutional Development, Research and Innovation of Thailand under Contracts No. B16F640076, No. B50G670107; Polish National Science Centre under Contract No. 2019/35/O/ST2/02907; Swedish Research Council under Contract No. 2019.04595; The Swedish Foundation for International Cooperation in Research and Higher Education under Contract No. CH2018-7756.

[1] L. G. Landsberg, Sov. Phys. Usp. **28**, 435 (1985).
[2] L. G. Landsberg, Phys. Rep. **128**, 301 (1985).
[3] C. J. Fan and J. K. He, Phys. Rev. D **109**, 074003 (2024).
[4] T. Barnes, S. Godfrey, and E. S. Swanson, Phys. Rev. D **72**, 054026 (2005).
[5] S. Navas *et al.* (Particle Data Group), Phys. Rev. D **110**, 030001 (2024).
[6] M. Ablikim *et al.* (BESIII Collaboration), Phys. Rev. Lett. **111**, 242001 (2013).
[7] M. Ablikim *et al.* (BESIII Collaboration), Chin. Phys. C **48**, 093001 (2024).
[8] M. Ablikim *et al.* (BESIII Collaboration), Chin. Phys. C **39**, 093001 (2015).
[9] M. Ablikim *et al.* (BESIII Collaboration), Chin. Phys. C **45**, 103001 (2021).
[10] M. Ablikim *et al.* (BESIII Collaboration), Chin. Phys. C **46**, 113002 (2022).
[11] M. Ablikim *et al.* (BESIII Collaboration), Chin. Phys. C **46**, 113003 (2022).
[12] M. Ablikim *et al.* (BESIII Collaboration), Phys. Rev. D **106**, 072007 (2022).
[13] M. Ablikim *et al.* (BESIII Collaboration), Phys. Rev. Lett. **104**, 132002 (2010).
[14] S. Dobbs *et al.* (CLEO Collaboration), Phys. Rev. Lett. **101**, 182003 (2008).
[15] P. Rubin *et al.* (CLEO Collaboration), Phys. Rev. D **72**, 092004 (2005).
[16] M. Ablikim *et al.* (BESIII Collaboration), Nucl. Instrum. Methods Phys. Res., Sect. A **614**, 345 (2010).
[17] M. Ablikim *et al.* (BESIII Collaboration), Chin. Phys. C **44**, 040001 (2020).
[18] S. Agostinelli *et al.* (GEANT4 Collaboration), Nucl. Instrum. Methods Phys. Res., Sect. A **506**, 250 (2003).
[19] D. J. Lange, Nucl. Instrum. Methods Phys. Res., Sect. A **462**, 152 (2001).
[20] See Supplemental Material at http://link.aps.org/supplemental/10.1103/PhysRevD.110.L111101 for generator for $h_c \to e^+e^-\eta_c$.
[21] R. G. Ping, Chin. Phys. C **32**, 599 (2008).
[22] R. L. Yang, R. G. Ping, and H. Chen, Chin. Phys. Lett. **31**, 061301 (2014).
[23] M. Ablikim *et al.* (BESIII Collaboration), Phys. Rev. Lett. **132**, 181901 (2024).
[24] M. Ablikim *et al.* (BESIII Collaboration), Phys. Rev. Lett. **132**, 101801 (2024).
[25] M. Ablikim *et al.* (BESIII Collaboration), Phys. Rev. Lett. **131**, 191802 (2023).
[26] M. Ablikim *et al.* (BESIII Collaboration), Phys. Rev. Lett. **130**, 251902 (2023).
[27] M. Ablikim *et al.* (BESIII Collaboration), Phys. Rev. Lett. **131**, 141802 (2023).
[28] M. Ablikim *et al.* (BESIII Collaboration), Phys. Rev. Lett. **130**, 151904 (2023).
[29] Z. R. Xu and K. L. He, Chin. Phys. C **36**, 742 (2012).
[30] M. Ablikim *et al.* (BESIII Collaboration), Phys. Rev. D **106**, 072007 (2022).
[31] M. Ablikim *et al.* (BESIII Collaboration), Phys. Rev. D **96**, 111101(R) (2017).
[32] M. Ablikim *et al.* (BESIII Collaboration), Phys. Rev. D **83**, 112005 (2011).
[33] M. Ablikim *et al.* (BESIII Collaboration), Phys. Rev. D **89**, 092008 (2014).
[34] M. Ablikim *et al.* (BESIII Collaboration), Eur. Phys. J. C **76**, 369 (2016).
[35] M. Ablikim *et al.* (BESIII Collaboration), Chin. Phys. C **40**, 113001 (2016).
[36] M. Gell-Mann and F. Zachariasen, Phys. Rev. **124**, 953 (1961).

M. Ablikim,[1] M. N. Achasov,[10,c] P. Adlarson,[67] S. Ahmed,[15] M. Albrecht,[4] R. Aliberti,[28] A. Amoroso,[66a,66c] M. R. An,[32] Q. An,[63,49] X. H. Bai,[57] Y. Bai,[48] O. Bakina,[29] R. Baldini Ferroli,[23a] I. Balossino,[24a] Y. Ban,[38,k] K. Begzsuren,[26] N. Berger,[28] M. Bertani,[23a] D. Bettoni,[24a] F. Bianchi,[66a,66c] J. Bloms,[60] A. Bortone,[66a,66c] I. Boyko,[29] R. A. Briere,[5] H. Cai,[68] X. Cai,[1,49] A. Calcaterra,[23a] G. F. Cao,[1,54] N. Cao,[1,54] S. A. Cetin,[53a] J. F. Chang,[1,49] W. L. Chang,[1,54] G. Chelkov,[29,b] D. Y. Chen,[6] G. Chen,[1] H. S. Chen,[1,54] M. L. Chen,[1,49] S. J. Chen,[35] X. R. Chen,[25] Y. B. Chen,[1,49] Z. J. Chen,[20,l] W. S. Cheng,[66c] G. Cibinetto,[24a] F. Cossio,[66c] X. F. Cui,[36] H. L. Dai,[1,49] X. C. Dai,[1,54] A. Dbeyssi,[15] R. E. de Boer,[4] D. Dedovich,[29] Z. Y. Deng,[1] A. Denig,[28] I. Denysenko,[29] M. Destefanis,[66a,66c] F. De Mori,[66a,66c] Y. Ding,[33] C. Dong,[36] J. Dong,[1,49] L. Y. Dong,[1,54] M. Y. Dong,[1,49,54] X. Dong,[68] S. X. Du,[71] Y. L. Fan,[68] J. Fang,[1,49] S. S. Fang,[1,54] Y. Fang,[1] R. Farinelli,[24a] L. Fava,[66b,66c] F. Feldbauer,[4] G. Felici,[23a] C. Q. Feng,[63,49] J. H. Feng,[50] M. Fritsch,[4] C. D. Fu,[1] Y. Gao,[38,k] Y. Gao,[64] Y. Gao,[63,49] Y. G. Gao,[6] I. Garzia,[24a,24b] P. T. Ge,[68] C. Geng,[50] E. M. Gersabeck,[58] A. Gilman,[61] K. Goetzen,[11] L. Gong,[33] W. X. Gong,[1,49] W. Gradl,[28] M. Greco,[66a,66c] L. M. Gu,[35] M. H. Gu,[1,49] S. Gu,[2] Y. T. Gu,[13] C. Y. Guan,[1,54] A. Q. Guo,[22] L. B. Guo,[34] R. P. Guo,[40] Y. P. Guo,[9,h] A. Guskov,[29] T. T. Han,[41] W. Y. Han,[32] X. Q. Hao,[16] F. A. Harris,[56] N. Hüsken,[22,28] K. L. He,[1,54] F. H. Heinsius,[4] C. H. Heinz,[28] T. Held,[4] Y. K. Heng,[1,49,54] C. Herold,[51] M. Himmelreich,[11,f] T. Holtmann,[4] Y. R. Hou,[54] Z. L. Hou,[1] H. M. Hu,[1,54] J. F. Hu,[47,m] T. Hu,[1,49,54] Y. Hu,[1] G. S. Huang,[63,49] L. Q. Huang,[64] X. T. Huang,[41] Y. P. Huang,[1] Z. Huang,[38,k] T. Hussain,[65] W. Ikegami Andersson,[67] W. Imoehl,[22] M. Irshad,[63,49] S. Jaeger,[4] S. Janchiv,[26,j] Q. Ji,[1] Q. P. Ji,[16] X. B. Ji,[1,54] X. L. Ji,[1,49] Y. Y. Ji,[41] H. B. Jiang,[41] X. S. Jiang,[1,49,54] J. B. Jiao,[41] Z. Jiao,[18] S. Jin,[35] Y. Jin,[57] T. Johansson,[67] N. Kalantar-Nayestanaki,[55] X. S. Kang,[33] R. Kappert,[55] M. Kavatsyuk,[55] B. C. Ke,[43,1] I. K. Keshk,[4] A. Khoukaz,[60] P. Kiese,[28] R. Kiuchi,[1] R. Kliemt,[11] L. Koch,[30] O. B. Kolcu,[53a,e] B. Kopf,[4] M. Kuemmel,[4] M. Kuessner,[4] A. Kupsc,[67] M. G. Kurth,[1,54] W. Kühn,[30] J. J. Lane,[58] J. S. Lange,[30] P. Larin,[15] A. Lavania,[21] L. Lavezzi,[66a,66c] Z. H. Lei,[63,49] H. Leithoff,[28] M. Lellmann,[28] T. Lenz,[28] C. Li,[39] C. H. Li,[32] Cheng Li,[63,49] D. M. Li,[71] F. Li,[1,49] G. Li,[1] H. Li,[63,49] H. Li,[43] H. B. Li,[1,54] H. J. Li,[16] H. J. Li,[9,h] J. L. Li,[41] J. Q. Li,[4] J. S. Li,[50] Ke Li,[1] L. K. Li,[1] Lei Li,[3] P. R. Li,[31] S. Y. Li,[52] W. D. Li,[1,54] W. G. Li,[1] X. H. Li,[63,49] X. L. Li,[41] Xiaoyu Li,[1,54] Z. Y. Li,[50] H. Liang,[1,54] H. Liang,[63,49] H. Liang,[27] Y. F. Liang,[45] Y. T. Liang,[25] G. R. Liao,[12] L. Z. Liao,[1,54] J. Libby,[21] C. X. Lin,[50] B. J. Liu,[1] C. X. Liu,[1] D. Liu,[63,49] F. H. Liu,[44] Fang Liu,[1] Feng Liu,[6] H. B. Liu,[13] H. M. Liu,[1,54] Huanhuan Liu,[1] Huihui Liu,[17] J. B. Liu,[63,49] J. L. Liu,[64] J. Y. Liu,[1,54] K. Liu,[1] K. Y. Liu,[33] Ke Liu,[6] L. Liu,[63,49] M. H. Liu,[9,h] P. L. Liu,[1] Q. Liu,[54] Q. Liu,[68] S. B. Liu,[63,49] Shuai Liu,[46] T. Liu,[1,54] W. M. Liu,[63,49] X. Liu,[31] Y. Liu,[31] Y. B. Liu,[36] Z. A. Liu,[1,49,54] Z. Q. Liu,[41] X. C. Lou,[1,49,54] F. X. Lu,[16] F. X. Lu,[50] H. J. Lu,[18] J. D. Lu,[1,54] J. G. Lu,[1,49] X. L. Lu,[1] Y. Lu,[1] Y. P. Lu,[1,49] C. L. Luo,[34] M. X. Luo,[70] P. W. Luo,[50] T. Luo,[9,h] X. L. Luo,[1,49] S. Lusso,[66c] X. R. Lyu,[54] F. C. Ma,[33] H. L. Ma,[1] L. L. Ma,[41] M. M. Ma,[1,54] Q. M. Ma,[1] R. Q. Ma,[1,54] R. T. Ma,[54] X. X. Ma,[1,54] X. Y. Ma,[1,49] F. E. Maas,[15] M. Maggiora,[66a,66c] S. Maldaner,[4] S. Malde,[61] Q. A. Malik,[65] A. Mangoni,[23b] Y. J. Mao,[38,k] Z. P. Mao,[1] S. Marcello,[66a,66c] Z. X. Meng,[57] J. G. Messchendorp,[55] G. Mezzadri,[24a] T. J. Min,[35] R. E. Mitchell,[22] X. H. Mo,[1,49,54] Y. J. Mo,[6] N. Yu. Muchnoi,[10,c] H. Muramatsu,[59] S. Nakhoul,[11,f] Y. Nefedov,[29] F. Nerling,[11,f] I. B. Nikolaev,[10,c] Z. Ning,[1,49] S. Nisar,[8,i] S. L. Olsen,[54] Q. Ouyang,[1,49,54] S. Pacetti,[23b,23c] X. Pan,[9,h] Y. Pan,[58] A. Pathak,[1] P. Patteri,[23a] M. Pelizaeus,[4] H. P. Peng,[63,49] K. Peters,[11,f] J. Pettersson,[67] J. L. Ping,[34] R. G. Ping,[1,54] R. Poling,[59] V. Prasad,[63,49] H. Qi,[63,49] H. R. Qi,[52] K. H. Qi,[25] M. Qi,[35] T. Y. Qi,[9] T. Y. Qi,[2] S. Qian,[1,49] W. B. Qian,[54] Z. Qian,[50] C. F. Qiao,[54] L. Q. Qin,[12] X. P. Qin,[9] X. S. Qin,[41] Z. H. Qin,[1,49] J. F. Qiu,[1] S. Q. Qu,[36] K. H. Rashid,[65] K. Ravindran,[21] C. F. Redmer,[28] A. Rivetti,[66c] V. Rodin,[55] M. Rolo,[66c] G. Rong,[1,54] Ch. Rosner,[15] M. Rump,[60] H. S. Sang,[63] A. Sarantsev,[29,d] Y. Schelhaas,[28] C. Schnier,[4] K. Schoenning,[67] M. Scodeggio,[24a,24b] D. C. Shan,[46] W. Shan,[19] X. Y. Shan,[63,49] J. F. Shangguan,[46] M. Shao,[63,49] C. P. Shen,[9] P. X. Shen,[36] X. Y. Shen,[1,54] H. C. Shi,[63,49] R. S. Shi,[1,54] X. Shi,[1,49] X. D. Shi,[63,49] J. J. Song,[41] W. M. Song,[27,1] Y. X. Song,[38,k] S. Sosio,[66a,66c] S. Spataro,[66a,66c] K. X. Su,[68] P. P. Su,[46] F. F. Sui,[41] G. X. Sun,[1] H. K. Sun,[1] J. F. Sun,[16] L. Sun,[68] S. S. Sun,[1,54] T. Sun,[1,54] W. Y. Sun,[34] W. Y. Sun,[27] X. Sun,[20,l] Y. J. Sun,[63,49] Y. K. Sun,[63,49] Y. Z. Sun,[1] Z. T. Sun,[1] Y. H. Tan,[68] Y. X. Tan,[63,49] C. J. Tang,[45] G. Y. Tang,[1] J. Tang,[50] J. X. Teng,[63,49] V. Thoren,[67] Y. T. Tian,[25] I. Uman,[53b] B. Wang,[1] C. W. Wang,[35] D. Y. Wang,[38,k] H. J. Wang,[31] H. P. Wang,[1,54] K. Wang,[1,49] L. L. Wang,[1] M. Wang,[41] M. Z. Wang,[38,k] Meng Wang,[1,54] W. Wang,[50] W. H. Wang,[68] W. P. Wang,[63,49] X. Wang,[38,k] X. F. Wang,[31] X. L. Wang,[9,h] Y. Wang,[50] Y. Wang,[63,49] Y. D. Wang,[37] Y. F. Wang,[1,49,54] Y. Q. Wang,[1] Y. Y. Wang,[31] Z. Wang,[1,49] Z. Y. Wang,[1] Ziyi Wang,[54] Zongyuan Wang,[1,54] D. H. Wei,[12] P. Weidenkaff,[28] F. Weidner,[60] S. P. Wen,[1] D. J. White,[58] U. Wiedner,[4] G. Wilkinson,[61] M. Wolke,[67] L. Wollenberg,[4] J. F. Wu,[1,54] L. H. Wu,[1] L. J. Wu,[1,54] X. Wu,[9,h] Z. Wu,[1,49] L. Xia,[63,49] H. Xiao,[9,h] S. Y. Xiao,[1] Z. J. Xiao,[34] X. H. Xie,[38,k] Y. G. Xie,[1,49] Y. H. Xie,[6] T. Y. Xing,[1,54] G. F. Xu,[1]

Q. J. Xu,[14] W. Xu,[1,54] X. P. Xu,[46] Y. C. Xu,[54] F. Yan,[9,h] L. Yan,[9,h] W. B. Yan,[63,49] W. C. Yan,[71] Xu Yan,[46] H. J. Yang,[42,g] H. X. Yang,[1] L. Yang,[43] S. L. Yang,[54] Y. X. Yang,[12] Yifan Yang,[1,54] Zhi Yang,[25] M. Ye,[1,49] M. H. Ye,[7] J. H. Yin,[1] Z. Y. You,[50] B. X. Yu,[1,49,54] C. X. Yu,[36] G. Yu,[1,54] J. S. Yu,[20,l] T. Yu,[64] C. Z. Yuan,[1,54] L. Yuan,[2] X. Q. Yuan,[38,k] Y. Yuan,[1] Z. Y. Yuan,[50] C. X. Yue,[32] A. Yuncu,[53a,a] A. A. Zafar,[65] Y. Zeng,[20,l] B. X. Zhang,[1] Guangyi Zhang,[16] H. Zhang,[63] H. H. Zhang,[50] H. H. Zhang,[27] H. Y. Zhang,[1,49] J. J. Zhang,[43] J. L. Zhang,[69] J. Q. Zhang,[34] J. W. Zhang,[1,49,54] J. Y. Zhang,[1] J. Z. Zhang,[1,54] Jianyu Zhang,[1,54] Jiawei Zhang,[1,54] L. M. Zhang,[52] L. Q. Zhang,[50] Lei Zhang,[35] S. Zhang,[50] S. F. Zhang,[35] Shulei Zhang,[20,l] X. D. Zhang,[37] X. Y. Zhang,[41] Y. Zhang,[61] Y. H. Zhang,[1,49] Y. T. Zhang,[63,49] Yan Zhang,[63,49] Yao Zhang,[1] Yi Zhang,[9,h] Z. H. Zhang,[6] Z. Y. Zhang,[68] G. Zhao,[1] J. Zhao,[32] J. Y. Zhao,[1,54] J. Z. Zhao,[1,49] Lei Zhao,[63,49] Ling Zhao,[1] M. G. Zhao,[36] Q. Zhao,[1] S. J. Zhao,[71] Y. B. Zhao,[1,49] Y. X. Zhao,[25] Z. G. Zhao,[63,49] A. Zhemchugov,[29,b] B. Zheng,[64] J. P. Zheng,[1,49] W. J. Zheng,[1,54] Y. Zheng,[38,k] Y. H. Zheng,[54] B. Zhong,[34] C. Zhong,[64] L. P. Zhou,[1,54] Q. Zhou,[1,54] X. Zhou,[68] X. K. Zhou,[54] X. R. Zhou,[63,49] X. Y. Zhou,[32] A. N. Zhu,[1,54] J. Zhu,[36] K. Zhu,[1] K. J. Zhu,[1,49,54] S. H. Zhu,[62] T. J. Zhu,[69] W. J. Zhu,[36] W. J. Zhu,[9,h] Y. C. Zhu,[63,49] Z. A. Zhu,[1,54] B. S. Zou,[1] and J. H. Zou[1]

(BESIII Collaboration)

[1]*Institute of High Energy Physics, Beijing 100049, People's Republic of China*
[2]*Beihang University, Beijing 100191, People's Republic of China*
[3]*Beijing Institute of Petrochemical Technology, Beijing 102617, People's Republic of China*
[4]*Bochum Ruhr-University, D-44780 Bochum, Germany*
[5]*Carnegie Mellon University, Pittsburgh, Pennsylvania 15213, USA*
[6]*Central China Normal University, Wuhan 430079, People's Republic of China*
[7]*China Center of Advanced Science and Technology, Beijing 100190, People's Republic of China*
[8]*COMSATS University Islamabad, Lahore Campus, Defence Road, Off Raiwind Road, 54000 Lahore, Pakistan*
[9]*Fudan University, Shanghai 200443, People's Republic of China*
[10]*G.I. Budker Institute of Nuclear Physics SB RAS (BINP), Novosibirsk 630090, Russia*
[11]*GSI Helmholtzcentre for Heavy Ion Research GmbH, D-64291 Darmstadt, Germany*
[12]*Guangxi Normal University, Guilin 541004, People's Republic of China*
[13]*Guangxi University, Nanning 530004, People's Republic of China*
[14]*Hangzhou Normal University, Hangzhou 310036, People's Republic of China*
[15]*Helmholtz Institute Mainz, Johann-Joachim-Becher-Weg 45, D-55099 Mainz, Germany*
[16]*Henan Normal University, Xinxiang 453007, People's Republic of China*
[17]*Henan University of Science and Technology, Luoyang 471003, People's Republic of China*
[18]*Huangshan College, Huangshan 245000, People's Republic of China*
[19]*Hunan Normal University, Changsha 410081, People's Republic of China*
[20]*Hunan University, Changsha 410082, People's Republic of China*
[21]*Indian Institute of Technology Madras, Chennai 600036, India*
[22]*Indiana University, Bloomington, Indiana 47405, USA*
[23a]*INFN Laboratori Nazionali di Frascati, I-00044 Frascati, Italy*
[23b]*INFN Sezione di Perugia, I-06100 Perugia, Italy*
[23c]*University of Perugia, I-06100 Perugia, Italy*
[24a]*INFN Sezione di Ferrara, I-44122 Ferrara, Italy*
[24b]*University of Ferrara, I-44122 Ferrara, Italy*
[25]*Institute of Modern Physics, Lanzhou 730000, People's Republic of China*
[26]*Institute of Physics and Technology, Peace Ave. 54B, Ulaanbaatar 13330, Mongolia*
[27]*Jilin University, Changchun 130012, People's Republic of China*
[28]*Johannes Gutenberg University of Mainz, Johann-Joachim-Becher-Weg 45, D-55099 Mainz, Germany*
[29]*Joint Institute for Nuclear Research, 141980 Dubna, Moscow region, Russia*
[30]*Justus-Liebig-Universitaet Giessen, II. Physikalisches Institut, Heinrich-Buff-Ring 16, D-35392 Giessen, Germany*
[31]*Lanzhou University, Lanzhou 730000, People's Republic of China*
[32]*Liaoning Normal University, Dalian 116029, People's Republic of China*
[33]*Liaoning University, Shenyang 110036, People's Republic of China*
[34]*Nanjing Normal University, Nanjing 210023, People's Republic of China*
[35]*Nanjing University, Nanjing 210093, People's Republic of China*
[36]*Nankai University, Tianjin 300071, People's Republic of China*
[37]*North China Electric Power University, Beijing 102206, People's Republic of China*

[38]Peking University, Beijing 100871, People's Republic of China
[39]Qufu Normal University, Qufu 273165, People's Republic of China
[40]Shandong Normal University, Jinan 250014, People's Republic of China
[41]Shandong University, Jinan 250100, People's Republic of China
[42]Shanghai Jiao Tong University, Shanghai 200240, People's Republic of China
[43]Shanxi Normal University, Linfen 041004, People's Republic of China
[44]Shanxi University, Taiyuan 030006, People's Republic of China
[45]Sichuan University, Chengdu 610064, People's Republic of China
[46]Soochow University, Suzhou 215006, People's Republic of China
[47]South China Normal University, Guangzhou 510006, People's Republic of China
[48]Southeast University, Nanjing 211100, People's Republic of China
[49]State Key Laboratory of Particle Detection and Electronics, Beijing 100049, Hefei 230026, People's Republic of China
[50]Sun Yat-Sen University, Guangzhou 510275, People's Republic of China
[51]Suranaree University of Technology, University Avenue 111, Nakhon Ratchasima 30000, Thailand
[52]Tsinghua University, Beijing 100084, People's Republic of China
[53a]Turkish Accelerator Center Particle Factory Group, Istanbul Bilgi University, 34060 Eyup, Istanbul, Turkey
[53b]Near East University, Nicosia, North Cyprus, Mersin 10, Turkey
[54]University of Chinese Academy of Sciences, Beijing 100049, People's Republic of China
[55]University of Groningen, NL-9747 AA Groningen, The Netherlands
[56]University of Hawaii, Honolulu, Hawaii 96822, USA
[57]University of Jinan, Jinan 250022, People's Republic of China
[58]University of Manchester, Oxford Road, Manchester, M13 9PL, United Kingdom
[59]University of Minnesota, Minneapolis, Minnesota 55455, USA
[60]University of Muenster, Wilhelm-Klemm-Str. 9, 48149 Muenster, Germany
[61]University of Oxford, Keble Rd, Oxford, UK OX13RH
[62]University of Science and Technology Liaoning, Anshan 114051, People's Republic of China
[63]University of Science and Technology of China, Hefei 230026, People's Republic of China
[64]University of South China, Hengyang 421001, People's Republic of China
[65]University of the Punjab, Lahore-54590, Pakistan
[66a]University of Turin and INFN, University of Turin, I-10125, Turin, Italy
[66b]University of Eastern Piedmont, I-15121, Alessandria, Italy
[66c]INFN, I-10125, Turin, Italy
[67]Uppsala University, Box 516, SE-75120 Uppsala, Sweden
[68]Wuhan University, Wuhan 430072, People's Republic of China
[69]Xinyang Normal University, Xinyang 464000, People's Republic of China
[70]Zhejiang University, Hangzhou 310027, People's Republic of China
[71]Zhengzhou University, Zhengzhou 450001, People's Republic of China

[a]Also at Bogazici University, 34342 Istanbul, Turkey.
[b]Also at the Moscow Institute of Physics and Technology, Moscow 141700, Russia.
[c]Also at the Novosibirsk State University, Novosibirsk, 630090, Russia.
[d]Also at the NRC "Kurchatov Institute", PNPI, 188300, Gatchina, Russia.
[e]Also at Istanbul Arel University, 34295 Istanbul, Turkey.
[f]Also at Goethe University Frankfurt, 60323 Frankfurt am Main, Germany.
[g]Also at Key Laboratory for Particle Physics, Astrophysics and Cosmology, Ministry of Education; Shanghai Key Laboratory for Particle Physics and Cosmology; Institute of Nuclear and Particle Physics, Shanghai 200240, People's Republic of China.
[h]Also at Key Laboratory of Nuclear Physics and Ion-beam Application (MOE) and Institute of Modern Physics, Fudan University, Shanghai 200443, People's Republic of China.
[i]Also at Harvard University, Department of Physics, Cambridge, MA, 02138, USA.
[j]Currently at: Institute of Physics and Technology, Peace Ave.54B, Ulaanbaatar 13330, Mongolia.
[k]Also at State Key Laboratory of Nuclear Physics and Technology, Peking University, Beijing 100871, People's Republic of China.
[l]School of Physics and Electronics, Hunan University, Changsha 410082, China.
[m]Also at Guangdong Provincial Key Laboratory of Nuclear Science, Institute of Quantum Matter, South China Normal University, Guangzhou 510006, China.